# MODELING OF WHOLE FIELD VAPOR PRESSURE DURING REFLOW FOR FLIP CHIP BGA AND WIRE BOND PBGA PACKAGES

Tong Yan Tee, Xue-Jun Fan, and Thiam Beng Lim
Institute of Microelectronics
11 Science Park Road
Singapore Science Park II
Singapore 117685
Phone: (65) 7705411, Fax: (65) 7745747
Email: tongyan@ime.org.sg

## ABSTRACT

In this paper, FEA models are built for both flip chip BGA (FCBGA) and wire bond PBGA packages to predict the moisture distribution, followed by the calculation of vapor pressure distribution in the package using the micro-mechanics approach with consideration of the micro-void effect. Results show that the vapor pressure saturated much faster than the moisture diffusion, and a near uniform vapor pressure is reached in the package. The vapor pressure is strongly dependent on the temperature and its magnitude can't exceed the saturated pressure at the corresponding temperature, even when more moisture is added in. The vapor pressure introduces additional mismatch to the package besides the CTE thermal mismatch. Vapor pressure-induced expansion is directly related to the vapor pressure distribution, rather than the moisture distribution. Moisture desorption during reflow is also studied and it has significant effect on the moisture distribution, but not on the vapor pressure distribution.

## 1. INTRODUCTION

The moisture-induced failures, e.g., popcorn and delamination, of IC packages are common phenomenon during solder reflow. The failures are due to sudden vaporization of moisture absorbed by the package at high temperature condition. Therefore, it is critical to evaluate the strength of internal vapor pressure generated in the package during reflow. The popcorn failure was first postulated by Fukuzawa et al. [2] in 1985, and later supported by many publications [1, 3, 6-11].

JEDEC standard [5] is widely used to conduct reliability test on moisture sensitivity of the electronic packages. Kitano et al. [6] showed that the package cracking is not controlled by the absolute water weight gain, rather it is due to the local moisture concentration at the critical interface. Therefore, the moisture diffusion modeling is required. However, the modeling of ensuing vapor pressure within the package during the reflow is the key element in understanding the failure mechanism. Previous researchers [3, 6-8] assumed that the delamination exists before the reflow, and considered the vapor pressure as traction loading subjected to the delaminated interfaces. There were some studies done and a few methods were proposed to estimate the vapor pressure acting on the delaminated interface. Since the vapor pressure is generated anywhere in the package, it is necessary to investigate the whole field vapor pressure distribution before the package delamination.

## 2. VAPOR PRESSURE MODELING

For plastic materials such as mold compound, the saturated moisture concentration ($C_{sat}$) is a few orders larger than the corresponding saturated ambient water vapor density during the moisture preconditioning, e.g., $\rho_g$ at 85°C/85%RH (see Table 1). This implies that the moisture absorbed by plastic materials is partially condensed into water in the micro-voids or free-volume of the materials. During the reflow, the moisture vaporizes at high temperature and produces internal vapor pressure. The vapor pressure, however, will maintain at its saturated pressure as long as the moisture in the voids is not fully vaporized.

Table 1. Properties of moisture preconditioning for a typical mold compound

| Moisture Preconditioning | Saturated Vapor Density $\rho_g$ (g/cm$^3$) | Saturated Moisture Concentration $C_{sat}$ (g/cm$^3$) |
|---|---|---|
| 30°C/60%RH | $3.04\times10^{-5}$ | $7.86\times10^{-3}$ |
| 85°C/60%RH | $3.58\times10^{-4}$ | $8.84\times10^{-3}$ |
| 85°C/85%RH | $3.58\times10^{-4}$ | $1.25\times10^{-2}$ |

Here, the Representative Volume Element (RVE) approach is introduced to estimate the vapor pressure generated inside of the material. Let's take a very small representative material sample, termed RVE as shown in Fig.1 [4]. From the microscopic level, the RVE is large enough to be statistically representative of the material properties at this location. Therefore, a field quantity, the void volume fraction, $f$, can be defined as

$$f = \frac{dV_f}{dV} \tag{1}$$

where $dV_f$ is the void volume and $dV$ is the element volume, $0 \le f \le 1$. When $f$ = 1 (fully voided), it implies that the delamination occurs at this location. The void volume fraction is a field variable, and has different evolution at different locations. It evolves faster along the interface than inside the material if the interfacial adhesion is weak. However, the initial micro-voids are distributed randomly but uniformly in the material, thus the initial void volume fraction, $f_0$, is a material property.

A useful quantity, the moisture density in the voids, can be described as

$$\rho_m = \frac{dW_m}{dV_f} = \frac{dW_m / dV}{dV_f / dV} = \frac{C}{f_0} \tag{2}$$

where $dW_m$ is the moisture weight in a RVE. In addition, the transition temperature, $T_1$, can be defined [1] as the temperature at which the moisture in the voids is fully transformed to vapor phase,

$$\rho_m(x_i, T_0) = \rho_g(T_1) \tag{3}$$

where $\rho_g(T_1)$ is the saturated vapor density at temperature $T_1$, and $T_0$ is the preconditioning temperature at which the moisture is absorbed.

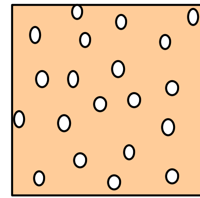

Fig. 1. A representative volume element (RVE)

It is assumed that the water vapor follows the ideal gas law. The vapor pressure can be calculated based on the local moisture concentration after preconditioning which determines the transition temperature, $T_1$. There are 3 distinct cases at which vapor pressure can be computed. The first case is when the moisture density in the voids is low enough such that all the moisture becomes vaporized at preconditioning temperature, $T_0$:

$$p = \frac{C\, p_g(T_0) T}{f\, \rho_g(T_0) T_0} \quad \text{when } T_1 \le T_0 \tag{4}$$

where $p$ is the pressure and $p_g$ is the saturated vapor pressure.

In the second case, the moisture is fully vaporized at a temperature between preconditioning temperature, $T_0$, and the peak reflow temperature, $T$:

$$p = \frac{p_g(T_1) T}{T_1} \quad \text{when } T_0 \le T_1 \le T \tag{5}$$

For the last case, the moisture is not fully vaporized even at reflow temperature, $T$:

$$p = p_g(T) \quad \text{when } T_1 \ge T \tag{6}$$

The initial void volume fraction, $f_0$, may be estimated from the material temperature-dependent moisture property. According to eq.

(2), when saturated, the local concentration, $C$, is same as $C_{sat}$. So, the initial void volume fraction can be expressed as following

$$f_0 = \frac{C_{\text{sat}}}{\rho_m} \qquad (7)$$

Since $\rho_m \approx 1.0\text{g/cm}^3$, we have

$$f_0 \approx C_{\text{sat}}\big|_{100°C/100\%RH} \qquad (8)$$

where 100°C/100%RH is selected as the near-saturated condition. Eq. (8) provides a simple way to predict the approximate magnitude of the voids existing in materials. The estimation is at the lower-limit since the moisture usually exists as a mixture of water and vapor at 100°C/100%RH. Table 2 lists the results of the initial void volume fraction for some commonly used plastic materials in IC packages, computed by eq. (8), using the moisture property data given by Galloway et al. [3]. It shows that the values are usually between 1% and 5 %.

Table 2. Initial void volume fraction for some common materials in IC packages

| Material | BT | Die Attach | Mold Compound | Solder Resist |
|---|---|---|---|---|
| $f_0$ (%) | 3.46 | 3.29 | 1.46 | 5.05 |

## 3. FEA MODEL

In order to calculate the vapor pressure during reflow after the moisture preconditioning, it is necessary to know the moisture concentration distribution in the package, according to eqs. (4-6). In FEA, the transient moisture diffusion is analogous to heat conduction, and it can be described by Fick's Law as

$$\frac{\partial^2 C^2}{\partial x^2} + \frac{\partial^2 C^2}{\partial y^2} + \frac{\partial^2 C^2}{\partial z^2} = \frac{1}{\alpha_D}\frac{\partial C}{\partial t} \qquad (9)$$

where $C$ is the local moisture concentration (g/cm$^3$), $x$, $y$, $z$ are the spatial coordinates (cm), $\alpha_D$ is the moisture diffusivity (cm$^2$/s), and $t$ is the time (s). Moisture wetness is used as the field variable as it is continuous across multi-material interface [7]. It is defined as

$$w = \frac{C}{C_{\text{sat}}} \qquad (10)$$

where $0 \le w \le 1$, $w$ = 0 means it is dry, and $w$ = 1 means it is saturated with moisture.

2D FEA half-models are generated for both unmolded FCBGA with depopulated array (156 I/O, 10x10mm chip, and 27x27mm BT substrate) and molded wire bond PBGA (35x35mm, 388 I/O, 2 layer). The element plots are shown in Fig 2 & 3 respectively. For moisture absorption modeling, the initial condition is $w$ = 0 for the whole package, and the boundary condition is $w$ = 1 at the external interfaces which are exposed to ambient moisture. The moisture properties of diffusivity ($D$) and $C_{sat}$ used in JEDEC level 1, 85%°C/85%RH, are listed in table 3. Die, copper, gold plate, and solder bump do not absorb moisture, and are assigned with very small values of diffusivity and solubility for FEA.

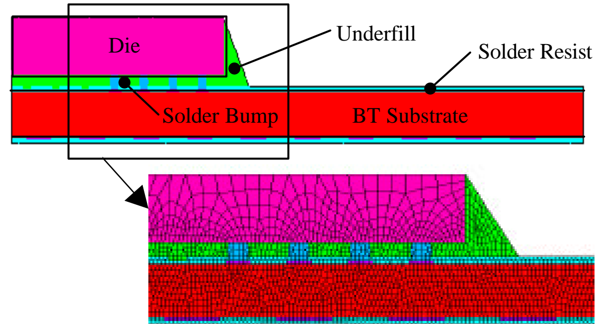


Fig 2. FEA model of FCBGA

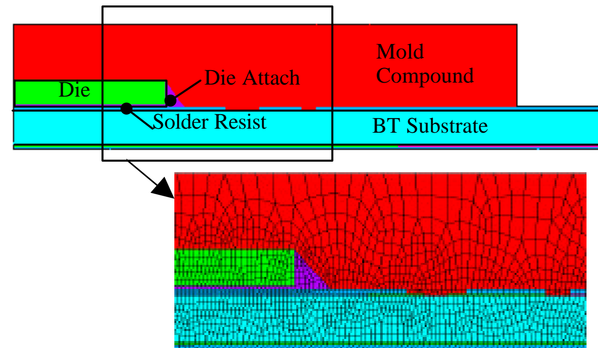


Fig 3. FEA model of wire bond PBGA

Table 3. Diffusivity and $C_{sat}$ used in the moisture diffusion modeling

| Material | Diffusivity $D$ (cm$^2$/s) | $C_{sat}$ (g/cm$^3$) |
|---|---|---|
| BT | 8.55e-9 | 2.40e-2 |
| Die Attach | 1.68e-7 | 5.30e-3 |
| Mold Compound | 5.40e-8 | 4.00e-3 |
| Solder Resist | 2.47e-8 | 3.88e-2 |
| Underfill | 5.60e-9 | 2.47e-2 |

Moisture desorption is considered because moisture content in the package is lost during reflow, and this may affect the moisture and vapor pressure distributions. For moisture desorption, the initial condition for the package is the moisture distribution after moisture preconditioning. The boundary condition is $w = 0$ at the exposed interfaces. The desorption conditions analyzed is 2 minutes at 220°C, which is the worst case in the typical reflow temperature profile of moisture sensitivity test. The $C_{sat}$ data used are the same, but the diffusivity values are assumed to be 100 times faster than in the moisture absorption at 85°C/85%RH.

With the moisture wetness distribution, the local moisture concentration can be obtained simply by using eq. (10). This will determine the magnitude of vapor pressure in the package at the desired temperature, i.e., 220°C peak reflow temperature, using eq. (4-6).

## 4. FEA RESULTS AND DISCUSSIONS

### 4.1 Transient Vapor Pressure Modeling

The FE results of vapor pressure for FCBGA at level 1, reflow temperature of 220°C, are shown in Fig. 4, with different times of moisture absorption. The corresponding moisture diffusion distributions are shown in Fig. 5.

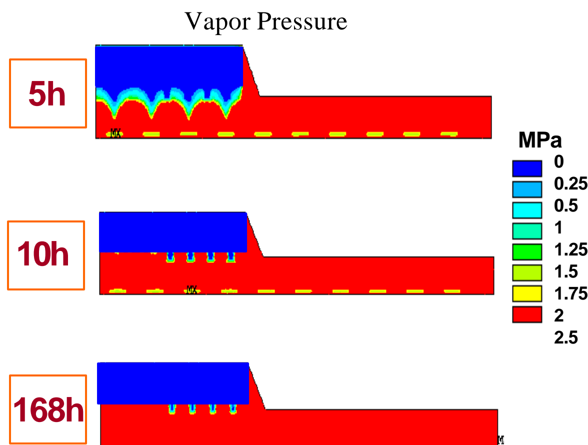


Fig. 4. Transient vapor pressure distribution in FCBGA at level 1, 220°C

It is found that moisture diffusion and vapor pressure have different distributions. The vapor pressure in the package saturated much faster than the moisture diffusion. At level 1 condition (168 hours), the package is almost fully saturated with vapor pressure of 2.32 MPa, which corresponds to $p_g$ at 220°C. Eq. (6) shows that the vapor pressure will remain its saturated pressure at 220°C when the transition temperature, $T_1$, is larger than 220°C. According to eq. (3), $T_1$ will be above 220°C as long as $\rho_m(T_0) \geq \rho_g(220°C) = 0.0116$ g/cm$^3$. Such a condition can be easily satisfied even though less moisture is absorbed.

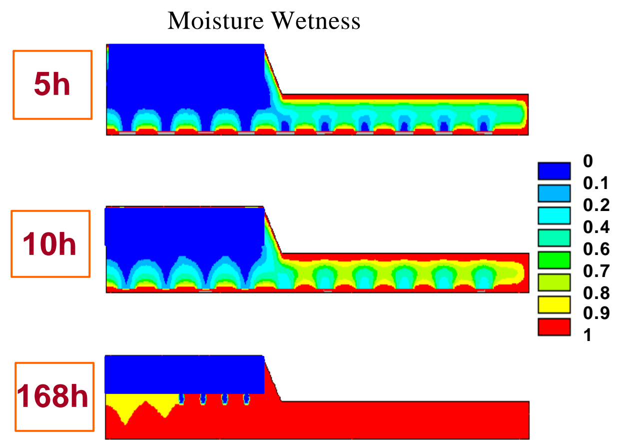


Fig. 5. Transient moisture distribution in FCBGA at level 1

Similarly, the vapor pressure distributions at 220°C for wire bond PBGA at level 3 are given in Fig. 6, with different times of moisture absorption. The corresponding moisture diffusion distributions are shown in Fig.7.

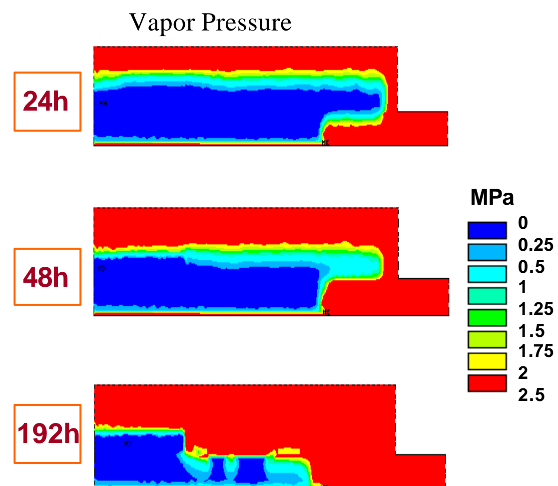


Fig. 6. Transient vapor pressure distribution in wire bond PBGA at level 3, 220°C

For wire bond PBGA, the moisture diffusion and vapor pressure also have different distributions. At level 3 (192 hours), the moisture diffusion is still far from saturation, but the vapor pressure is already saturated in more than half of the package. As a comparison, the moisture diffusion and the vapor pressure at level 1 condition (see Fig. 8) are much more saturated than in level 3 (see Fig. 6 & 7).

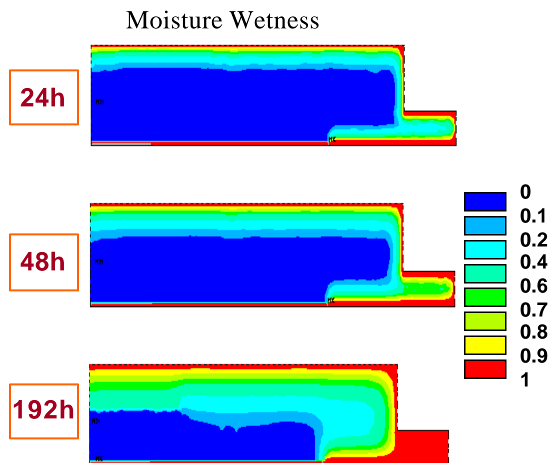


Fig. 7. Transient moisture distribution in wire bond PBGA at level 3

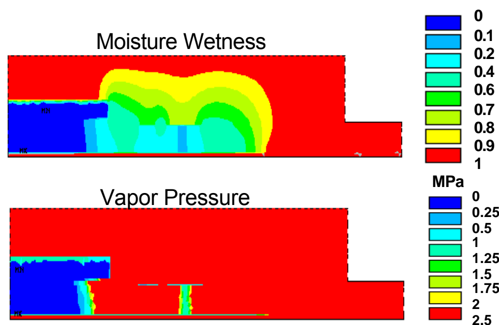


Fig. 8. Moisture and vapor pressure distribution in wire bond PBGA at level 1 (168 hours), 220°C

## 4.2 Effect of Moisture Desorption

The effect of moisture desorption during reflow on the vapor pressure distribution is studied. At high temperature, the moisture diffusivity for desorption is a few orders higher than the case for absorption at level 1. The consideration of moisture loss during reflow gives a more realistic vapor pressure calculation.

Fig. 9 & 10 show the vapor pressure and moisture diffusion distributions of FCBGA before and after 2 minutes of desorption at 220°C. The initial condition is level 1 (85°C/85%RH, 168 hours). It is found that the moisture desorption during reflow affects the moisture distribution, but not the vapor pressure distribution, especially in the region near the package exterior. The vapor pressure can't go beyond the saturated vapor pressure which has strong dependence on the temperature. Even though there is significant amount of moisture loss in the package during reflow, the moisture content is still large enough to produce the saturated vapor pressure at the reflow temperature.

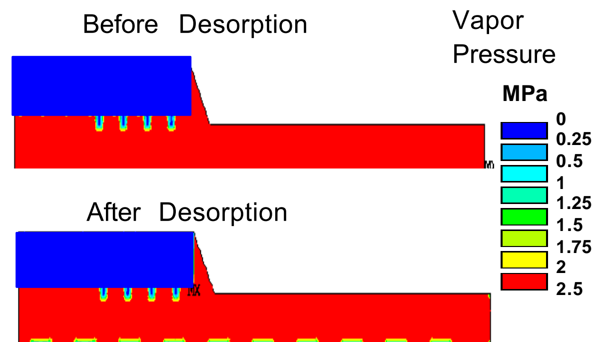


Fig. 9. Vapor pressure distribution in FCBGA before and after desorption

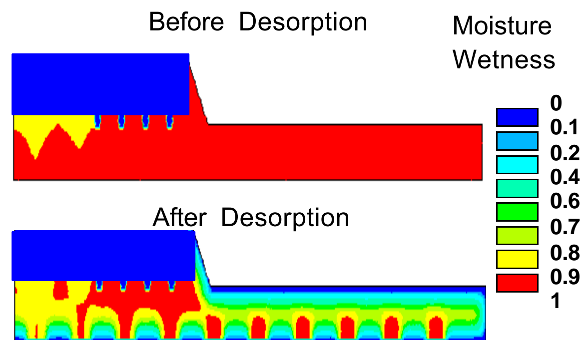


Fig. 10. Moisture distribution in FCBGA before and after desorption

Similar observations can also be found in wire bond PBGA for vapor pressure and moisture diffusion distributions during reflow with consideration of moisture desorption (see Fig. 11 & 12).

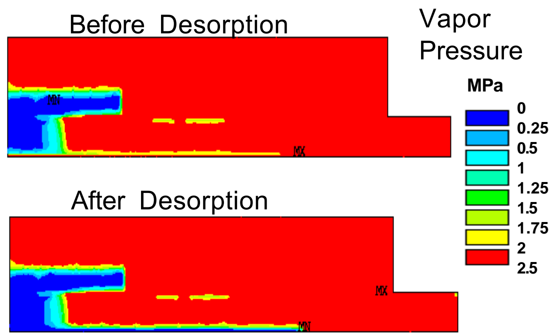


Fig. 11. Vapor pressure distribution in wire bond PBGA before and after desorption

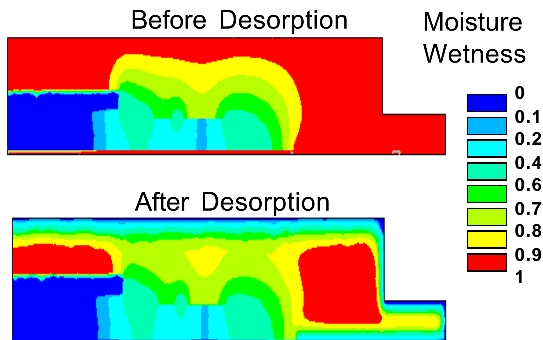


Fig. 12. Moisture distribution in wire bond PBGA before and after desorption

Again, the moisture distribution during reflow is affected by the moisture desorption, but the vapor pressure distribution is almost remain unchanged.

## 4.3 Effect of Initial Void Volume Fraction

The results above are based on the estimation of initial void volume fraction ($f_0$) by eq. (8) which underestimates the $f_0$ values. It is important to understand the effect of $f_0$ on the vapor pressure distribution. Fig. 13 & 14 show the results for FCBGA and wire bond PBGA respectively, with different values of $f_0$. Although the $f_0$ is doubled, but the vapor pressure distributions in both packages at 220°C after level-1 moisture absorption, are not much affected

When $f_0$ is doubled, the moisture properties ($D$ and $C_{sat}$) are assumed to be unchanged. The saturated vapor pressure can still be maintained in the packages because there is enough moisture content in the micro-voids, even the moisture density is halved by doubling the $f_0$. By using eq. (2) with $f_0$ of 10% (worst case), the minimum $C_{sat}$ required in the package to maintain the saturated pressure of 2.32MPa is 1.16 x $10^{-3}$ g/cm$^3$, which is much smaller than the $C_{sat}$ for typical mold compound listed in Table 1. Even though the vapor pressure is not sensitive to $f_0$, but the local moisture concentration in the package increases with higher $f_0$, which weakens the interfacial adhesion and makes it more susceptible to failures.

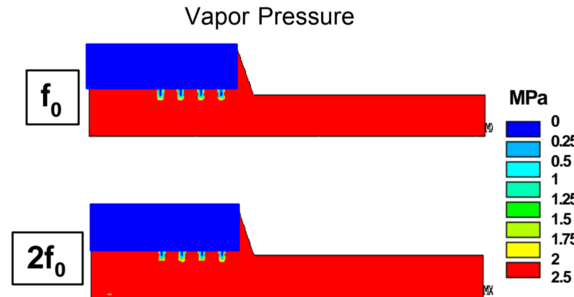


Fig 13. Effect of $f_0$ on the vapor pressure distribution of FCBGA

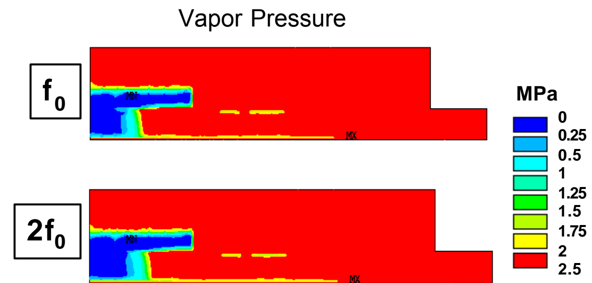


Fig 14. Effect of $f_0$ on the vapor pressure distribution of wire bond PBGA

## 4.4 Failure Mechanism

The moisture affects the package reliability at reflow from two aspects: generation of vapor pressure and degradation of interfacial adhesion. Fig. 15 shows the relative effect of moisture absorption on the interfacial adhesion and vapor pressure in the package. The interfacial adhesion is weakened with higher moisture level.

Previous results of vapor pressure estimation show that the saturated vapor pressure can be reached even with less moisture absorbed. For FCBGA and wire bond PBGA modeled here, the saturated pressure can be reached at the critical interface, even at the level 3 condition.

However, the interfacial adhesion will be significantly decreased with more moisture absorption. When the adhesion strength is reduced to the level below the vapor pressure, delamination will occur. Therefore, the knowledge of material interfacial adhesion strength with moisture effect at high temperature condition is important in determining the failure criteria.

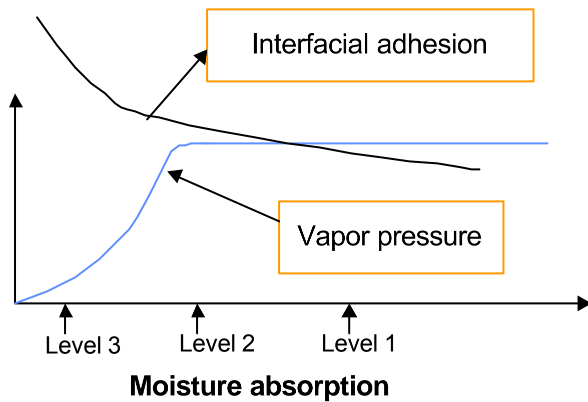


Fig. 15. Relative effect of moisture absorption on interfacial adhesion and vapor pressure

### 4.5 Vapor Pressure-Induced Expansion

The previous FEA results conclude that the vapor pressure saturated much faster than the moisture diffusion. This implies that the vapor pressure may be uniformly distributed in the plastic material regardless of moisture saturation. The Young's modulus of plastic material drops a few orders at the reflow temperature, thus the vapor pressure-induced expansion may become as important as thermal expansion. For instance, assume the Young's modulus of a typical underfill at 220°C is 500 MPa, and Poisson ratio is 0.3. Therefore, the volume change caused by vapor pressure, $P_g$(220°C) of 2.32 MPa, can be estimated as

$$\frac{\Delta V}{V} = \frac{1-2\boldsymbol{n}}{E} p = 1.856e-3 \qquad (11)$$

which is comparable with expansion due to the CTE thermal mismatch. It is obvious that the vapor pressure-induced expansion introduces additional mismatch. It must also be pointed out that such an expansion is directly related to the vapor pressure distribution, rather than the moisture distribution.

## 5. CONCLUSIONS

The package vapor pressure distribution during reflow is the key factor in understanding the failure mechanism. FEA moisture diffusion models are constructed for both FCBGA and wire bond PBGA packages to predict the local moisture concentration at the critical interfaces, which determines the magnitude of vapor pressure. The vapor pressure is found to be saturated much faster than the moisture diffusion. At reflow temperature, the moisture may not be fully vaporized after the level-1 moisture preconditioning, and thus saturated pressure is reached in most area of the FCBGA and wire bond PBGA packages. The vapor pressure generated can never go beyond the saturated pressure at the corresponding temperature, e.g., pressure of 2.32 MPa at 220°C. The vapor pressure is strongly temperature dependent. Moisture desorption affects the moisture distribution, rather than the vapor pressure distribution.

The moisture affects the package reliability at reflow from two aspects: generation of vapor pressure and degradation of interfacial adhesion. Although the vapor pressure remains at its saturated pressure when more moisture is absorbed, the adhesion strength may continuously deteriorate with additional moisture. When the interfacial adhesion is reduced to the level below the vapor pressure, the delamination will occur. The initial void volume fraction has insignificant effect on the vapor pressure distribution because there is always sufficient moisture concentration in the package to maintain the saturated pressure. However, larger void volume fraction along the interface will weaken the adhesion strength and make it more susceptible to failures.

The vapor pressure induces additional mismatch to the package, which is of the same order as the CTE thermal mismatch. This vapor pressure-induced expansion is directly related to the vapor pressure distribution, rather than the moisture distribution. Therefore, it is important to consider the mismatch caused by vapor pressure in the stress modeling.

## REFERENCES


1. Fan, X.J. and Lim, T.B., 1999, "Mechanism Analysis for the Moisture Induced Failures in IC Packages," ASME International Mechanical Engineering Congress & Exposition, 11th Symposium of Mechanics of Surface Mount Assemblies, IMECE/EPE-14, Tennessee, Nashville, November 14-19, 1999
2. Fukuzawa, I., Ishiguro, S., and Nanbu, S., 1985, "Moisture Resistance Degradation of Plastic LSI's by Reflow Soldering," Proc. IRPS, pp. 192-197.
3. Galloway, J.E. and Miles, B.M., 1997, "Moisture Absorption and Desorption Predictions for Plastic Ball Grid Array Packages," IEEE Tranasction on Component,Packaging, and Manufacturing, A, 20(3), pp. 274-279.
4. Gurson, A.L., 1977, ASME Journal of Applied Mechanics, 99, pp. 2.
5. JEDEC Standard, 1994, Test method A 112, Moisture Induced Stress Sensitivity for Plastic Surface Mount Devices, Electronic Industries Association.
6. Kitano, M., Nishimura, A., and Kawai, S., 1988, "Analysis of Package Cracking during Reflow Soldering Process," Proc. IRPS, pp. 90-95.
7. Tay, A.A.O. and Lin, T., 1996, "Moisture Diffusion and Heat Transfer in Plastic IC Packages," IEEE Tranasction on Component, Packaging, and Manufacturing, A, 19(2), pp. 186-193.
8. Wong, E.H. and Lim, T.B., 1998, "Moisture Diffusion and Vapor Pressure Modeling in IC Packaging," 48th ECTC, pp. 1372-1378.
9. Yi, Sung, Goh, J. S. and Yang, J. C., 1997, "Residual Stresses in Plastic IC Packages During Surface Mounting Process Preceded by Moisture Soaking Test," IEEE Transactions on Components, Packaging, and Manufacturing Technology, B, Vol. 20, No. 3, pp. 247-255.
10. Yi, S., Goh, J. S. and Yang, J. C., 1995, "Finite Element Analysis of Hygrothermally Induced Stresses in Plastic Packages," Proceedings of 5th International Symposium on the Physical and Failure Analysis of Integrated Circuits (IPFA-95), pp. 11-16.
11. Yi, Sung and Yue, Chee Yoon, 1998, "Hygrothermally Induced Residual Stresses in a Plastic BGA", Proceedings of the 1998 Workshop on Mechanical Reliability of Polymeric Materials and Plastic Packages of IC Devices", ASME, pp. 271-275.